MSUCL-209
April 1976

A Measurement of Γ_{rad}/Γ for the 7.654 MeV State of ^{12}C and the Rate of the Stellar 3α Reaction*

R.G. Markham, Sam M. Austin and M.A.M. Shahabuddin

Cyclotron Laboratory and Physics Department
Michigan State University, East Lansing, Michigan 48824

ABSTRACT

The branching ratio Γ_{rad}/Γ for the radiative de-excitation of the 7.654 MeV, 0^+ state in ^{12}C has been measured. Coincidences between α particles from $^{12}C(\alpha,\alpha')^{12}C$(7.654 MeV) and recoil ^{12}C ions at the proper energy and angle were the signature of radiative decay. Conservative techniques were used throughout to avoid the need for large corrections. A value of $\Gamma_{rad}/\Gamma = (3.87\pm0.25) \times 10^{-4}$ was obtained in good agreement with other recent results but substantially higher than the previously accepted value of $(2.9\pm0.3) \times 10^{-4}$. Available results are reviewed and a recommended value of Γ_{rad}/Γ is presented. The implication of this result for the rate of the 3α process in stellar helium burning is discussed and a recommended reaction rate is presented.

NUCLEAR STRUCTURE: ^{12}C, 7.654 MeV state; measured Γ_{rad}/Γ. Stellar helium burning.

*Research supported by the U.S. National Science Foundation.

I. INTRODUCTION

After hydrogen has been converted to ^4He in the core of a star, the core contracts until temperatures sufficient to fuse ^4He into ^{12}C via the 3α reaction are reached. The $^{12}C(\alpha,\gamma)^{16}O$ reaction then converts part of the ^{12}C to ^{16}O, the extent of the conversion depending on the relative rates of the two reactions. When the 3α reaction is relatively fast, ^{12}C is the main product of helium burning; and when it is relatively slow, ^{16}O is dominant.[1] Since the subsequent evolution of a star greatly depends on the ratio of ^{12}C to ^{16}O in the ashes of helium burning, it also depends in effect on a knowledge of the rates of the 3α and $^{12}C(\alpha,\gamma)^{16}O$ reactions. The rate of the latter reaction is still rather uncertain[2] and as we shall see recent measurements have cast doubt on the 3α rate as well.

In the 3α reaction ^4He is converted into ^{12}C via a two stage process

$$^4He + {}^4He \rightleftarrows {}^8Be \qquad {}^8Be + {}^4He \rightleftarrows {}^{12}C(7.654\ MeV) \rightarrow {}^{12}C(g.s.) + 2\gamma(e^+ + e^-)$$

where the arrows denote an equilibrium situation. The rate $p_{3\alpha}$ for this process depends on the Q value of the reaction and the width Γ_{rad} for γ-ray plus pair decay of the 7.654 MeV state leading eventually to the ground state of ^{12}C. Specifically[1]

$$P_{3\alpha} = n_\alpha^3 \hbar^5 \left(\frac{2\pi\sqrt{3}}{kTM_\alpha}\right)^3 \Gamma_{rad} e^{-Q/kT} \quad cm^{-3}sec^{-1} \qquad (1)$$

where n_α is the number density of α particles, M_α is the atomic mass of ^4He, k is Boltzman's constant and T is the temperature. A recent determination[3] of Q, accurate to ±0.2 keV has essentially

eliminated the contribution of the uncertainty in Q to that in $P_{3\alpha}$, but Γ_{rad} is less well known.

No direct measurements are available, and this width is obtained from the relationship

$$\Gamma_{rad} = \frac{\Gamma_{rad}}{\Gamma} \cdot \frac{\Gamma}{\Gamma_{\pi}} \cdot \Gamma_{\pi} \qquad (2)$$

The pair emission width of the state Γ_{π} is known to ±6% from inelastic electron scattering leading to this state[4] and Γ/Γ_{π} has been measured to accuracy of ±30%.[5] The ratio Γ_{rad}/Γ was thought to be well known until the recent measurement of Chamberlin, et al.[6] gave $(4.20\pm0.22) \times 10^{-4}$, nearly 45% higher than the previously accepted value of $(2.9\pm0.3) \times 10^{-4}$ [7] and a discrepancy of 3.5 standard deviations.

Since this discrepancy was the dominant uncertainty in $P_{3\alpha}$ we undertook the measurement described here. To lessen the chance of introducing systematic uncertainties such as have apparently affected at least one earlier experiment, we have employed a conservative experiment design (described in Section II) intended to minimize corrections to the raw data. Unfortunately these procedures also result in a relatively low event rate which is, hopefully, compensated by the reliability of the result.

Since this experiment was begun three other results have become available.[8-10] These are compared with the present value of Γ_{rad}/Γ in Section IV.

II. EXPERIMENTAL METHOD

A. General

The basic technique is similar to that used by Chamberlin, et al.[6] Inelastic alpha scattering is used to populate the 7.65

MeV state and the coincidence between a scattered alpha and a stable ^{12}C recoil is taken as the signature of radiative decay of the state. If the recoil detector is sufficiently large and placed at the kinematically defined angle, the branching ratio Γ_{rad}/Γ is just the ratio of the number of coincidence events to the total number of inelastic-alpha events leading to the population of the 7.65 MeV state.

In practice our technique differed from that of ref. 6 in the use of a higher energy beam (40.2 MeV) and a much more elaborate recoil detector consisting of a ΔE-E counter telescope with position sensitivity in two dimensions. This counter permitted a redundant identification of the recoil ions (by ΔE-E and position as well as time of flight) yielding a low background, and insured proper alignment of the detector through use of the position information. In order to avoid geometrical efficiency corrections the detector was placed close enough to the target to accept the entire recoil cone. During data taking the counting rates were kept sufficiently low to obviate the use of pile-up rejectors and the subtle, not always small, effects they may have on the relative efficiency for single and coincident events.[8] Finally, the singles and coincident events were event recorded without distinction so as to avoid the possibility of different counting losses for the two types of events.

A measurement of Γ_{rad}/Γ for the decay of the 4.44 MeV state in ^{12}C served as a check on the efficiency of the system, since this state always decays radiatively. In the present circumstances the recoil angle and energy of the ^{12}C ion are only

slightly different for the excitation of the 4.44 and 7.65 states (see Table I), so the comparison should be quite accurate.

B. Detectors

The recoil-detector telescope shown in Fig. 1 consists of a gas-filled proportional counter for ΔE_C and a silicon surface-barrier detector for E_C. The body of the detector is of one piece construction and houses the silicon detector (Ortec 400 mm^2 heavy-ion type) and the proportional counter chamber. The front window, about 125 $\mu g/cm^2$ in thickness, was constructed of multiple layers of formvar stretched over 25 μm diameter Wolfram support wires spaced 1.48 mm apart. It was coated on one side with a thin layer of gold to produce a conducting front cathode for the proportional counter; the front surface of the silicon detector serves as the rear cathode. The gas filling was 90% Argon + 10% Methane at 0.1 atm pressure. Fresh gas was continuously flowed through the counter with the pressure accurately maintained by a Cartesian manostat. The recoil angle (position) was determined by resistive charge division of the current signal on an anode wire with a resistance of 950 ohms. The out-of-plane angle (position) was inferred from the time difference between the signal from the stopping detector and that from the proportional counter. This time difference is due mainly to the drift time of the electrons from the ionization track to the anode wire lying just outside the irradiated volume.

In early experiments we discovered that secondary electrons from the target were able to penetrate the detector

entrance window and seriously degrade operation of the proportional counter. This problem was overcome by mounting a copper tube on the face of the detector and surrounding it with permanent magnets. Further details are given in ref. 11.

The alpha detector was a cooled silicon surface barrier detector with an active area of 150 mm^2 and a depletion depth of 1000 μm. A circular aperture of 12.3 mm diameter and a stepped absorber were placed ahead of the detector. The stepped absorber was constructed of multiple layers of 2.5 μm thick mylar foils placed so as to compensate for the variation of alpha energy with angle.

C. Electronics and Data Recording

A schematic drawing of the electronics is shown in Fig. 2. Charge sensitive preamps were used throughout. Signals from the two surface barrier detectors were sent to both fast and slow amplifiers. Time derivation was by leading-edge discrimination of the fast amplifier output. The time-of-flight TAC was started on the alpha detector time signal and stopped on the carbon detector time signal. True-start rates and stop rates were monitored and kept at about 200 Hz and 10 kHz respectively. The start discriminator level was set high to avoid unnecessary TAC dead time. The TAC output was sent to ADC-2 and the outputs of the slow amplifiers were sent to ADC-1 and 3 for the alpha energy and carbon stopping-energy, respectively.

The signals from the ends of the proportional counter anode wire were added, amplified and sent to ADC-4. The signal from the high angle end was separately amplified and sent to

ADC-5. All ADC's were gated open whenever an alpha energy signal was received corresponding to excitation of ^{12}C to 12 MeV or less. In this way singles and coincident events were handled in exactly the same manner with no possibility of different dead times.

Although counting losses were expected to be small because of the modest counting rates, as an additional check a pulser system was set up to inject pulses into each preamplifier. The number of pulses (at a constant rate of 1Hz) injected was scaled and compared to the number of pulser events found on playback of the data tapes.

Not shown in the Fig. 2 is the electronics associated with measurement of the out-of-plane angle (vertical position on the recoil detector). This was accomplished by starting a TAC on either the alpha detector or stopping detector (for coincidence or singles events respectively) and stopping it on the ΔE_C signal. Time derivation was obtained from the zero crossing of the bipolar outputs of the slow amplifiers. Because only five ADC's were available this information could not be recorded on tape during the final data taking runs.

In the setup phase data was recorded in two dimensional arrays and analyzed crudely on line to ensure proper operation of the system. During the actual data runs the data was recorded event by event on magnetic tape. All events whether coincident or single were recorded as five parameters, a zero being recorded if no pulse was received for a particular ADC.

E. Procedure

The initial step in the experimental procedure was the alignment of beam and detectors. The alpha detector was set at a peak in the inelastic scattering cross section at 53.4° in the lab and the recoil detector angle was varied until the recoils from population of the 4.44 MeV state were centered on the detector. A small recoil angle correction (0.5°) from the predicted angle was noted and used to correct the angle readout scale. Vertical alignment of the system was accomplished by moving the beam vertically until the coincident recoils from the 4.44 state were centered vertically on the recoil detector. To ensure that the alignment remained stable and to determine counting efficiency, check runs on the 4.44 MeV state were interspersed with data runs.

In addition to the 100 $\mu g/cm^2$ thick carbon target (enriched to 99.9% in ^{12}C) the following targets were used to identify possible contaminants: ^{13}C of ~200 $\mu g/cm^2$ thickness, Melamine of ~25 $\mu g/cm^2$ thickness on a formvar backing, and W_2O_3 of ~150 $\mu g/cm^2$ thickness. Runs on these targets were sandwiched between ^{12}C runs.

The beam current was maintained at 200 to 250 nA to keep the counting rates at constant, moderate levels. A summary of the experimental parameters is given in Table I.

III. DATA PROCESSING

A. Event Sorting

Following the experiment all coincidence events were copied to disk to simplify later sorting, and a singles-plus-coincidence

E_α spectrum was generated. The disk events were played back and two-dimensional spectra of ΔE_C-E_C, TOF-E_C and θ-E_C were generated subject to E_α being appropriate for the population of the 7.65 MeV state. With this gating the ^{12}C recoils could easily be distinguished from events due to the detection of one, two or three of the breakup alphas in the ΔE_C-E_C spectrum. Boundaries in the ΔE_C-E_C plane were then established, the events were resorted subject to the conditions on E_α and ΔE_C-E_C and boundaries were established in the TOF-E_C plane. The final boundary, in the θ-E_C plane, was more difficult to define because of a substantial number of events at the small angle side of the recoil detector. These events were from true coincidences with alphas scattering from the 4.44 MeV state, but with energy registered as appropriate for population of the 7.65 MeV state, i.e. they appeared in the "tail" of the 4.44 MeV α peak. Because the kinematic cone for these events is centered at larger angles only a fraction of these recoils falls on the detector and they are located on the larger angle side. The θ-E_C boundary was defined to discriminate against these "4.44 tail" events, maintaining essentially 100% efficiency for the 7.65 MeV events. The angular width of the recoil cone for the 7.65 MeV events was measured to be 1.5±0.1° FWHM; the width of the θ boundary used (and observed to contain essentially all events) was 5.8° and the total detector width was 7.2°. The angular width for the 4.44 MeV state was 1.56±0.07° FWHM which is not significantly different than that for the 7.65 MeV state. Thus, the efficiency measured for the 4.44 MeV state will be essentially the same as that for the 7.65 MeV state.

Having defined the boundaries, the E_α requirement was lifted and the entire set of event tapes was reprocessed. In this search of the tapes each two dimensional spectrum was generated subject only to the condition that the event satisfied the boundaries of the other complementary two dimensional spectra. Two E_α spectra were generated; one for events satisfying the boundaries in all three planes and one for all the other events. These two dimensional and E_α spectra are shown in Figs. 3 and 4. The coincidence E_α spectrum is dominated by events from the 7.65 MeV and 4.4 MeV states. The 4.4 MeV events were not fully excluded by the detector placement and θ-E_C boundaries. Note, however, that the total absence of the elastic group assures us that the true-to-random ratio is very high for the 7.65 MeV state.

B. Coincidence Efficiency

The coincidence efficiency was determined by measuring Γ_{rad}/Γ for the 4.44 MeV state using the two-dimensional boundaries from the 7.65 state analysis. These boundaries were modified only by translating the TOF-E_C boundaries to larger values of TOF, (necessary because of leading edge timing in the α channel), and by shifting the E_C boundaries by about 0.25 MeV (see Table I). This should be a valid test for counting losses because for a fixed scattering angle the recoil ions have very nearly the same energy and a predictably different recoil angle. All but 5.3 ±0.8% of the 4.4 MeV inelastic events also satisfied the recoil criteria. The great bulk of these losses are accounted for by the presence of the window support wires, 2.6±0.3%, and by pileup distortions, 2.6±1.3%. The estimate of window-support-wire losses is based on the diameter and

spacing of the wires. Pile-up losses were evaluated by comparison of the number of known pulser events and the number of pulser events satisfying reasonable two dimensional boundaries. An independent estimate of these losses was made by inspection of the signals present during random sampling. This was accomplished by construction of the two dimensional spectra subject only to E_α being appropriate for elastic scattering. The results for the ΔE_C and E_C spectra were approximately 2.5% pile up losses. Additional losses due to TAC, ADC, computer and discriminator dead times (already contained in the loss estimates for the pulser) are calculated to be small fractions of one per cent.

The final result for the coincidence efficiency is 0.947±0.008, the uncertainty being essentially statistical in nature.

C. Background Events

A small number of background events appear in the coincident E_α spectrum in the region of the 7.65 MeV group. Because the recoil ion is identified uniquely to be a carbon ion, the possibilities for contaminant induced background events are limited (except for ^{13}C) to inelastic excitation of the contaminant to a state which particle decays to carbon. Direct evaluation of background yields were obtained by performing the experiment with targets of ^{13}C, ^{14}N (melamine) and ^{16}O (W_2O_3) and processing the data in the same manner as for the 7.65 MeV state. The coincident yields from these experiments were then scaled by the ratio of the number of elastic scatterings from each contaminant as seen in the contaminant experiment and in the

7.65 MeV experiment. The results show that ^{13}C produces negligible background but ^{14}N and ^{16}O contribute 3.2±0.4% and 6±1% respectively, of the coincident events. The E_α spectrum with background subtracted is shown in Fig. 5. A comparison of this spectrum with the lower spectrum in Fig. 4 verifies the accuracy of the background subtraction.

D. Determination of Γ_{rad}/Γ

Table II summarizes the results. Using the three two-dimensional boundaries of Fig. 3 and E_α channel limits just enclosing the 7.65 MeV group as shown on Fig. 4 we find 261±16 coincident events with 24±3 of these attributed to contaminants and 14±2 additional events lost. The net result is

$$\frac{\Gamma_{rad}}{\Gamma} = (3.87\pm0.25)\times10^{-4}$$

The quoted uncertainty contains small contributions from the uncertainty in the coincidence efficiency and the dependence of the result on the choice of boundaries but is dominated by the statistical error.

The boundaries used in the determination were quite generous having been drawn to include essentially all points tentatively identified with the 7.6 inelastic group. The analysis was repeated with more restrictive boundaries with the same result for Γ_{rad}/Γ within 2%. Our ability to use loose boundaries is a consequence of the four-fold redundancy of the recoil identification.

IV. DISCUSSION

The results of the present experiment are compared with other values of Γ_{rad}/Γ in Table III. With the single exception of the result of Seeger and Kavanagh,[12] all values are consistent with each other and with the weighted mean of all the results. Thus, this result must either represent a rather large statistical fluctuation or be influenced by an undetected error. We have chosen to exclude the Seeger and Kavanagh value in forming the recommended weighted average. As can be seen from Table III the effect of this exclusion is about one-and-one-half times the estimated uncertainty for the weighted average. The sample standard deviation calculated from the five recent results with errors <0.4 (again excluding that of Seeger and Kavanagh) is 0.16, somewhat less than the uncertainty quoted for any of the experiments, lending credence to these error assignments.

In order to obtain Γ_{rad}, we use Eq. 2 with values of the widths given in Table IV to obtain.

$$\Gamma_{rad} = (3.61\pm1.13)\times10^{-3} \text{ eV} \qquad (3)$$

In their recent review Fowler, Caughlan and Zimmerman (FCZII)[15] tabulate a quantity $N_a^2\langle\alpha\alpha\alpha\rangle$ which is related to $P_{3\alpha}$ by

$$N_a^2\langle\alpha\alpha\alpha\rangle = 6\,\frac{N_a^2}{n_\alpha^3}\,P_{3\alpha}(\text{cm}^6\text{sec}^{-1}\text{mole}^{-2})$$

where N_a is Avagadro's number.

Using the values from Table IV yields

$$N_a^2\langle\alpha\alpha\alpha\rangle = \frac{2.74\times10^{-8}}{T_9^3}\exp(-4.4026/T_9). \qquad (4)$$

In Eq. 1 and here we have ignored the contribution of the 9.64 MeV state of ^{12}C. The result of Eq. 4 is related to the rate tabulated of FCZII by

$$N_a^2\langle\alpha\alpha\alpha\rangle = N_a^2\langle\alpha\alpha\alpha\rangle_{FCZII}\times0.913\,\exp(0.0083/T_9) \qquad (5)$$

Part of the change in the multiplicative constant results from the inclusion of the recent data of Strehl[16] in the determination of Γ_π.

Present sources of uncertainty in $P_{3\alpha}$ are tabulated in Table IV. It is clear that the uncertainty in Γ_π/Γ presently dominates the overall uncertainty of about 31% in the reaction rate. Fortunately at least two measurements of this quantity are presently in progress.[18,19]

Quantitative studies of the effect of changes in the reaction rates on ^{12}C production have been made by Arnett.[20] Combining his results with the reaction rates they obtained for the $^{12}C(\alpha,\gamma)^{16}O$ reaction, Dyer and Barnes[2] concluded that ^{12}C is the dominant product of helium burning, at least for stars with masses less than about 15 times the solar mass. While there are still substantial uncertainties in both $P_{3\alpha}$ and, especially, in the rate for $^{12}C(\alpha,\gamma)^{16}O$[2] it seems likely this conclusion will stand.

ACKNOWLEDGMENTS

The authors are grateful to C.N. Davids for making available a program for the calculation of three-body kinematics.

REFERENCES

1. See, Principles of Stellar Evolution and Nucleosynthesis, by D.D. Clayton (McGraw Hill, New York, 1968) and references therein.
2. P. Dyer and C.A. Barnes, Nucl. Phys. A233(1974)495 and references therein.
3. J.A. Nolen and S.M. Austin, Phys. Rev. C (to be published).
4. F. Ajzenberg-Selove, Nucl. Phys. A248(1975)1.
5. D.E. Alburger, Phys. Rev. 118(1960)235; A.W. Obst, T.B. Grandy and J.L. Weil, Phys. Rev. C5(1972)738.
6. D. Chamberlin, D. Bodansky, W.W. Jacobs and D.L. Oberg, Phys. Rev. C9(1964)69.
7. F. Ajzenberg-Selove and T. Lauritsen, Nucl. Phys. A114 (1968)1.
8. C.N. Davids, R.C. Pardo and A.W. Obst, Phys. Rev. C11(1975) 2063.
9. H.B. Mak, H.C. Evans, G.T. Ewan, A.B. McDonald and T.K. Alexander, Phys. Rev. 12(1975)1158.
10. A.W. Obst and W.J. Braithwaite, unpublished.
11. R.G. Markham, S.M. Austin and H. Laumer, Nucl. Instr. and Meth. 129(1975)141.
12. P.A. Seeger and R.W. Kavanagh, Nucl. Phys. 46(1963)577.
13. D.E. Alburger, Phys. Rev. 124(1961)193.
14. I. Hall and N.W. Tanner, Nucl. Phys. 53(1964)673.
15. W.A. Fowler, G.R. Caughlan, and B.A. Zimmerman, Annual Rev. of Astronomy and Astrophysics 13(1975)69.

16. P. Strehl, Z. Physik 234(1970)416.
17. H. Crannell,T.A. Griffy, L.R. Suelzle and M.R. Yearian, Nucl. Phys. A90(1967)152.
18. R.G.H. Robertson, R.A. Warner and S.M. Austin (unpublished).
19. D. E. Alburger, private communication.
20. W.D. Arnett , Astrophysics J. 176(1972)681.

FIGURE CAPTIONS

Fig. 1.--Schematic cross section of the counter telescope: (a) window frame, (b) front cover plate, (c) surface barrier detector, (d) bulkhead feed through, (e) anode wire.

Fig. 2.--Schematic diagram of the electronics used.

Fig. 3.--Two dimensional spectra of events with E_α appropriate for the 7.65 MeV state. The events in each spectrum are also subject to the requirement that they lie within the enclosed regions in the other two spectra. The diameter of each point is proportional to the number of events it represents with the smallest points representing one event. The points labelled "4.44" in the θ-E_c spectrum are from the tail of the 4.44 MeV state. Those labelled 3α in the ΔE_c-E_c spectrum arise when the three α particles from breakup of the 7.65 MeV state all pass through the detector.

Fig. 4.--The E_α spectra for all events (upper spectrum) and those satisfying the two dimensional constraints of Fig. 3 (lower spectrum). The arrows indicate the limits used to evaluate the branching ratio.

Fig. 5.--Background subtracted E_α peak for the 7.65 MeV state. Events are subject to the boundaries shown in Fig. 3. Background spectra were obtained from the contaminant runs and normalized by scaling to the elastic contaminant groups in the data run.

TABLE I.--Experimental Parameters.

Detector	State (MeV)	Lab. Angle(deg)	Solid Angle(msr)[a]	Distance (cm)	Lab Energy (MeV)
^{4}He	7.65	-53.4	3.0	20	23.49
	4.44	-53.4	3.0	20	26.46
^{12}C	7.65	+48.3	12.7	15	9.06[b]
	4.44	+51.5	12.7	15	9.30[b]

[a]Circular defining aperture.

[b]Mean energy less by about 350 keV due to energy losses in the target.

TABLE II.--Summary of Present Results.

Item	Number	Uncertainty
Events accepted	261	±16
Contaminant correction	-24	± 3
Efficiency correction	+14	± 2
Total	251	±16
Singles Events	647999	±805
Γ_{RAD}/Γ	3.87×10^{-4}	$\pm 0.25 \times 10^{-4}$

TABLE III.--Summary of Information in Γ_{rad}/Γ.

Identification Number	$\frac{\Gamma_{rad}}{\Gamma} \times 10^4$	Reference
1	3.4 ±0.9	Alburger[13]
2	2.82±0.29	Seeger and Kavanagh[12]
3	3.5 ±1.2	Hall and Tanner[14]
4	4.20±0.22	Chamberlin, et al.[6]
5	4.30±0.20	Davids, et al.[8]
6	4.15±0.34	Mak, et al.[9]
7	4.05±0.27	Obst and Braithwaite[10]
8	3.87±0.25	Present experiment
1-8[a]	3.96±0.10	Weighted average of all results
1,3-8[a]	4.12±0.11	Recommended weighted average

[a]The weighted average is calculated using the total quoted uncertainties of the individual measurements.

TABLE IV.--Parameters of the 3α Reaction Rate.

Parameter	Value	Contribution to uncertainty in $P_{3\alpha}$ (%)
Γ_π	$(60.5\pm3.9)\times10^{-b}$ eV [a]	6
Γ_π/Γ	$(6.9\pm2.1)\times10^{-6}$ [b]	30
Γ_{rad}/Γ	$(4.12\pm0.11)\times10^{-4}$ [c]	3
Γ_{rad}	$(3.61\pm1.13)\times10^{-3}$ eV [d]	31
Q	379.38±0.20 keV [e]	2 [f]
Total		31

[a] Refs. 16,17.
[b] Ref. 5. This is the only available measurement of Γ_π/Γ.
[c] Table III.
[d] Calculated from Eq. 2.
[e] Ref. 3.
[f] At T_9=0.1.

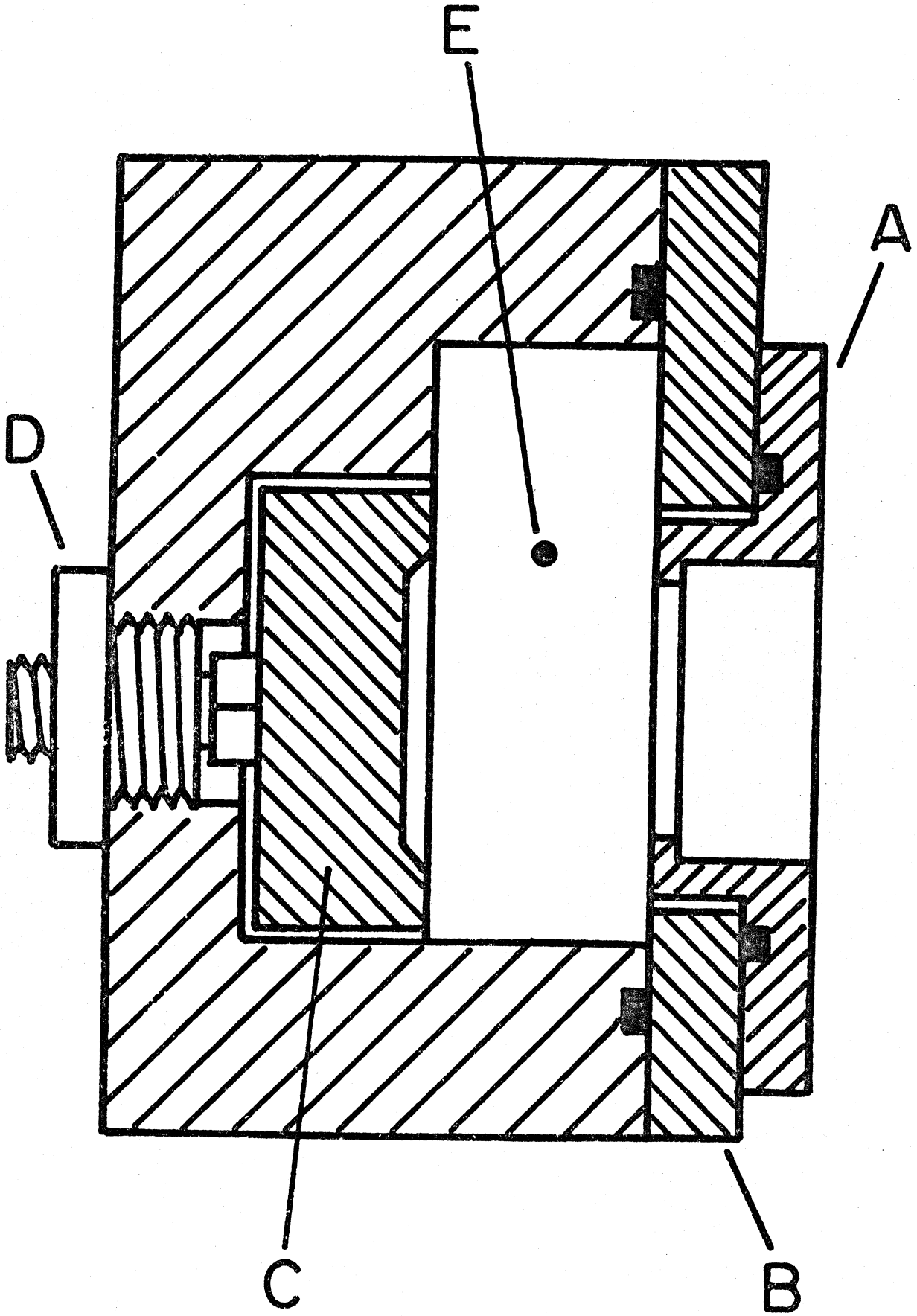
E
A
D
C
B

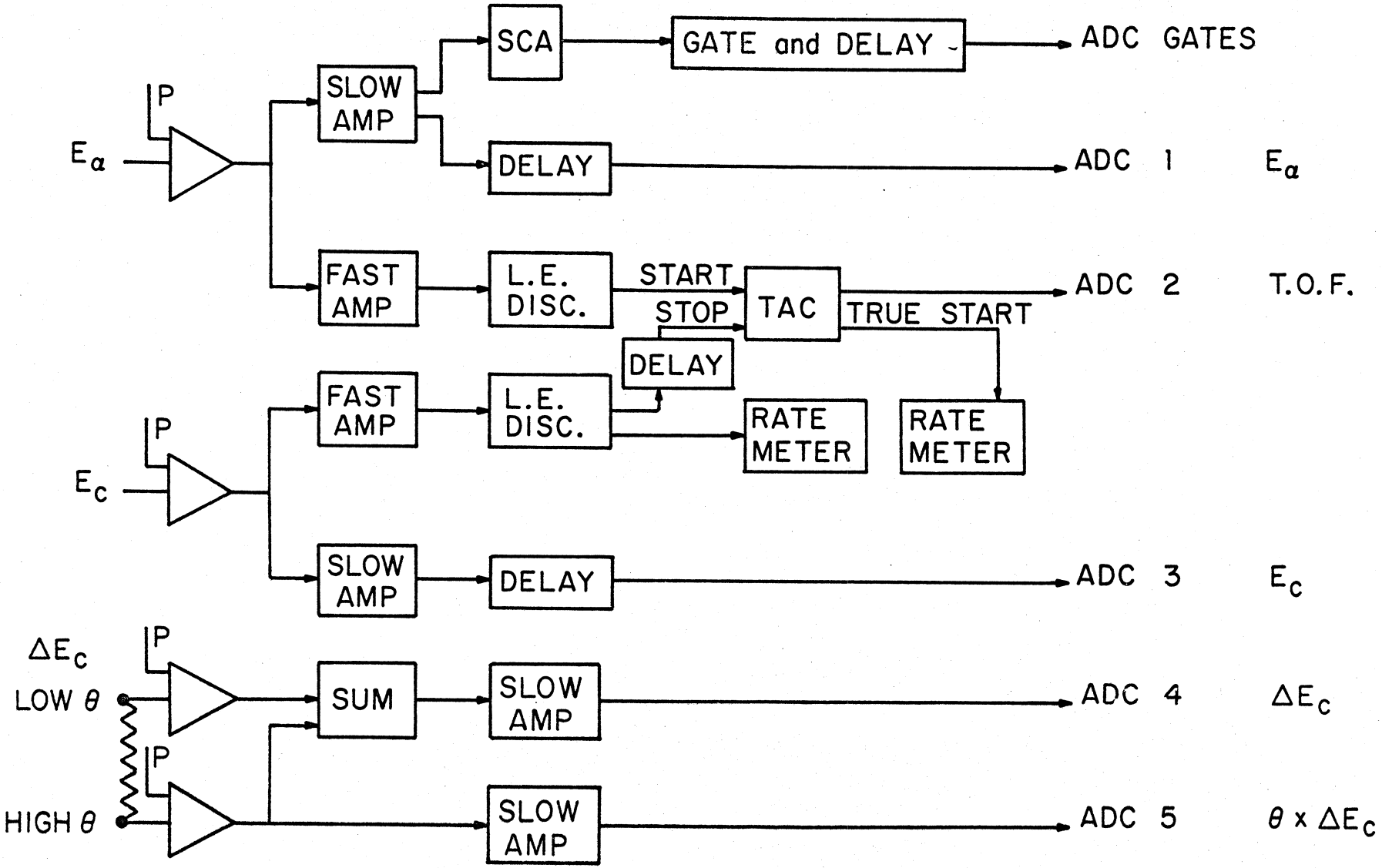
SCA
GATE and DELAY
ADC GATES
P
SLOW AMP
E_α
DELAY
ADC 1
E_α
FAST AMP
L.E. DISC.
START
STOP
TAC
TRUE START
ADC 2
T.O.F.
DELAY
FAST AMP
L.E. DISC.
RATE METER
RATE METER
P
E_c
SLOW AMP
DELAY
ADC 3
E_c
ΔE_c
LOW θ
P
SUM
SLOW AMP
ADC 4
ΔE_c
P
HIGH θ
SLOW AMP
ADC 5
$\theta \times \Delta E_c$

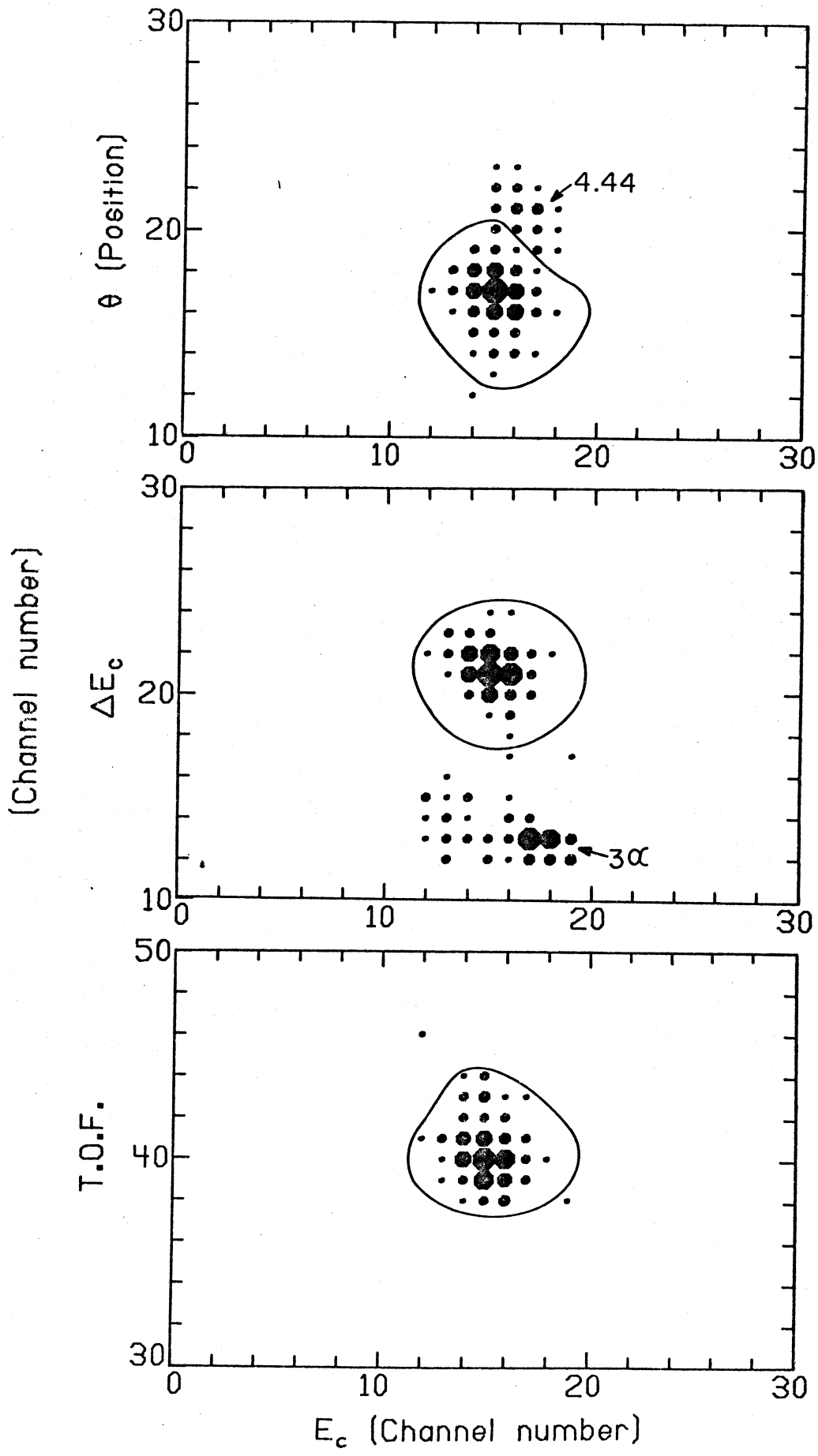
30
20
10
θ (Position)
4.44
0
10
20
30
ΔEc
3α
50
40
T.O.F.
(Channel number)
Ec (Channel number)

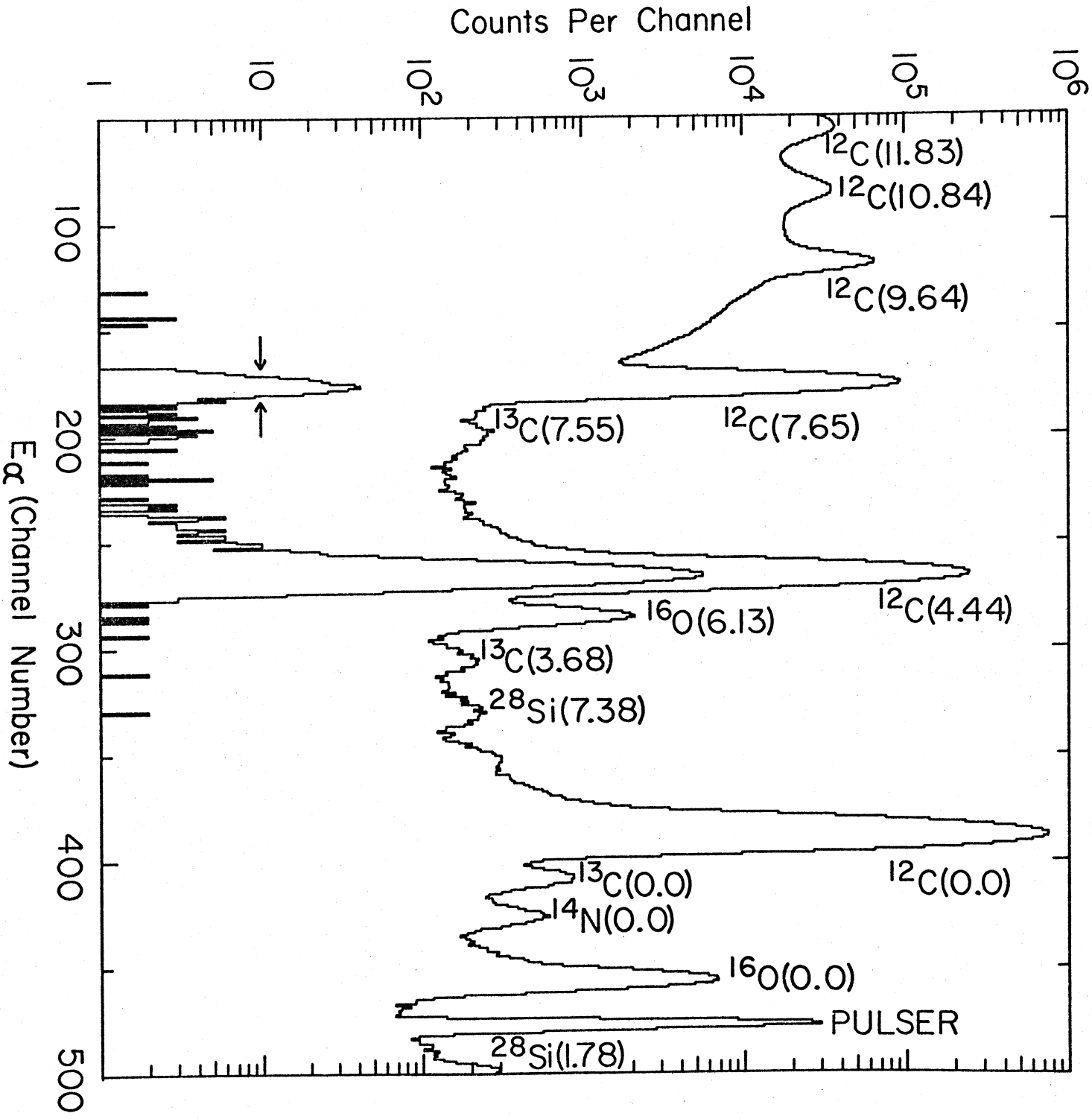
Counts Per Channel
1
10
10^2
10^3
10^4
10^5
10^6
Eα (Channel Number)
100
200
300
400
500
12C(11.83)
12C(10.84)
12C(9.64)
12C(7.65)
13C(7.55)
12C(4.44)
16O(6.13)
13C(3.68)
28Si(7.38)
12C(0.0)
13C(0.0)
14N(0.0)
16O(0.0)
PULSER
28Si(1.78)

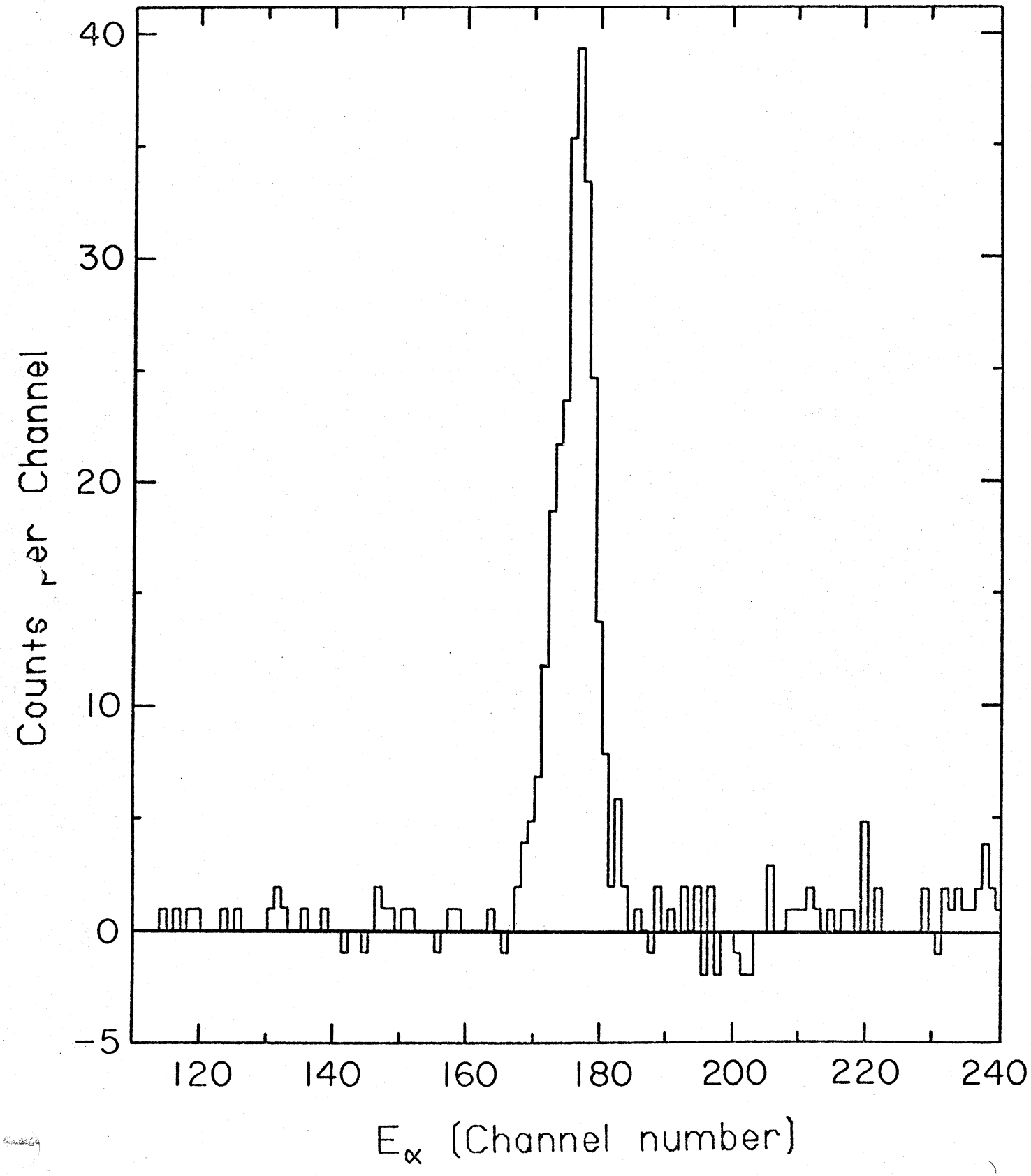
40
30
20
10
0
-5
Counts per Channel
120
140
160
180
200
220
240
E_α (Channel number)